Earth Planet. Sci. Lett. 692 (2026) 120247

Contents lists available at ScienceDirect

Earth and Planetary Science Letters

journal homepage: www.elsevier.com/locate/epsl

H_2O-poor minerals in equilibrium with volatile-bearing fluids: Insights from diamond-hosted mineral inclusions

Andrea Curtolo [a,b,*], Maxwell C. Day [b], Thomas Stachel [c], Martha G. Pamato [b], Fabrizio Nestola [b], Ingrid L. Chinn [d], Davide Novella [b]

[a] Bayerisches Geoinstitut, Universität Bayreuth, Bayreuth, 95447, Germany
[b] Dipartimento di Geoscienze, Università degli Studi di Padova, Padova, 35131, Italy
[c] Department of Earth and Atmospheric Sciences, University of Alberta, Edmonton, Canada
[d] De Beers Mining and Discovery, 144 Oxford Road, Johannesburg, 2196, South Africa

ARTICLE INFO

Editor: DR J BADRO

Keywords:
Diamond
Inclusions
H_2O
Canada
COH fluids
Thermodynamic model

ABSTRACT

We investigated the H_2O content of 21 garnet and clinopyroxene inclusions extracted from Canadian diamonds using Fourier Transform Infrared (FTIR) spectroscopy. Garnets have H_2O contents below the FTIR detection limit, while clinopyroxene inclusions have H_2O contents ranging from below the detection limit to 289 wt.ppm. These H_2O contents are lower than in the same minerals found in xenoliths from the same localities, supporting the idea that the activity of H_2O may be low during diamond formation, as previously suggested for samples from other localities (e.g., the Kalahari and Siberian cratons).

Considering these findings, both the speciation of COH fluid in the lithosphere and the incorporation of H in nominally anhydrous minerals were thermodynamically modelled along cratonic mantle geotherms to investigate the composition of diamond-forming fluids. The COH speciation model shows that, contrary to what has been previously suggested, diamonds are unlikely to form from a fluid at, or close to, the water maximum, as such conditions require oxygen fugacities higher than those expected in the lithospheric diamond stability field (log fO_2 (ΔIW) from +2 to 0 at ~8 GPa). The H incorporation modelling shows that to produce inclusions with the H_2O content detected here and elsewhere (dry to hundreds of ppm wt), fluids with low H_2O activity are required. The different H incorporation mechanisms relevant for each mineral will lead to variable H_2O contents, explaining the range observed here. These results indicate that lithospheric monocrystalline diamonds may form mainly from carbonatitic or hydrous-carbonated silicate melts rather than aqueous fluids.

1. Introduction

Diamonds represent one of the few means by which the deep Earth can be directly studied. The hard and chemically inert nature of diamond allows preservation of mineral and fluid inclusions which provide invaluable information about the otherwise inaccessible mantle. Inclusions in diamonds have been intensively studied over the last ~60 years providing crucial mineralogical and petrological information about the deep Earth (Stachel et al., 2022a and references therein). Apart from minerals and fluids, diamonds also incorporate N and H (among other impurities) into their crystal structure (Stachel et al., 2022b; Day et al., 2023). Investigation of the content and isotopic composition of such impurities has drastically improved our understanding of crust-mantle recycling of volatiles.

Diamond is a metasomatic mineral that forms from different carbon-oxygen-hydrogen (COH)-bearing fluid phases in the mantle (Shirey et al., 2013). Therefore, the study of diamonds can provide insights into the properties, compositions and sources of these fluids. This is especially important as fluid phases, given their mobility, can efficiently transport high concentrations of incompatible elements, refertilizing regions of the mantle and producing enriched mantle domains that can be geophysically detected (e.g., Eeken et al., 2018). Our understanding of diamond-forming fluids in the lithosphere is largely based on the study of fluid inclusions in fluid-rich diamonds, which are commonly referred to as fibrous diamonds (see, e.g., Weiss et al., 2022 and references therein). Such inclusions consist of residual low-density fluids and daughter mineral phases crystallized from the original high-density fluids (HDFs). Fibrous diamonds, however, are a particular type of

* Corresponding author.
E-mail address: Andrea.Curtolo@uni-bayreuth.de (A. Curtolo).

https://doi.org/10.1016/j.epsl.2026.120247
Received 14 January 2026; Received in revised form 25 June 2026; Accepted 20 July 2026
Available online 30 July 2026
0012-821X/© 2026 The Authors. Published by Elsevier B.V. This is an open access article under the CC BY license (http://creativecommons.org/licenses/by/4.0/).

diamond whose formation mechanisms are likely different from those of gem-quality (non-fibrous) diamonds.

In this regard, work on natural, gem-quality diamonds (e.g., Jablon and Navon, 2016; Krebs et al., 2019; Stachel et al., 2022a and references therein), along with experimental investigations of diamond formation (e.g., Luth et al., 2022), has helped elucidate the role of low-density fluids as well as carbonatitic and silicic melts in the formation of lithospheric *gem* diamonds. Several studies have investigated the H_2O content of diamond-hosted nominally anhydrous mineral (NAM) inclusions (see e.g., Matsyuk et al., 1998; Novella et al., 2015; Taylor et al., 2016; Curtolo et al., 2025a and references therein). Water contents of mineral inclusions were thought to preserve the original H_2O content of the mantle, as opposed to xenoliths where H_2O content was assumed to reflect different degrees of metasomatism (e.g., Doucet et al., 2014). However, given the fast diffusivity of H in minerals, the H_2O content of diamond-hosted NAM inclusions is unlikely to be representative of the original H_2O content of the lithosphere and, instead, likely reflects the H_2O content and activity of the diamond-forming fluid (see Curtolo et al., 2025a). Therefore, despite not providing direct information on the hydration state of the deep subcontinental lithosphere, the study of H_2O in diamond-hosted NAMs can provide unique insights into Earth's deep-water cycle and the composition of diamond-forming fluids.

Previous studies on the H_2O content of NAM inclusions focused mostly on specimens from Africa and Russia. Despite Canada being one of the most important diamond producers in the world (e.g., Curtolo et al. 2023), the H_2O content of only one olivine inclusion from Canada has been analyzed (Matveev and Stachel, 2009). Measuring the H_2O content of NAM inclusions hosted in Canadian diamonds is particularly important to address the possibility of sampling bias related to over-representation of diamonds from particular localities (i.e., Africa and Russia) and associated mantle environments (Curtolo et al., 2025a). Moreover, in previous studies, the composition and H_2O content of fluids were only discussed qualitatively, and the stability and thermodynamic properties of the phases involved in diamond formation have not been evaluated.

In this study, the H_2O content of 18 garnet and three clinopyroxene inclusions extracted from Canadian lithospheric diamonds was determined using FTIR spectroscopy. These samples are the first garnet and clinopyroxene inclusions from Canadian diamonds for which H_2O contents have been measured. The H_2O content of the mineral inclusions is compared to the H_2O content observed in the same minerals from mantle xenoliths from Canadian kimberlites. Thermodynamic models describing the speciation of COH fluids along a mantle geotherm and the incorporation of H in NAMs equilibrating with such fluids are provided. This allowed the nature of diamond-forming fluids, and the degree of H re-equilibration between mineral inclusions and such fluids, to be constrained.

2. Materials and methods

2.1. Samples

The H_2O content of 21 NAM inclusions, already extracted from their host diamonds, was determined. The samples are from the Diavik and Gahcho Kué diamond mines, Slave craton, Canada (Table 1, Fig. 1). Geochemical characteristics of the host diamonds and major element compositions of the inclusions are reported in Table 1 and S1 (Donnelly et al., 2007; Siva-Johty, 2020).

Samples include ten peridotitic garnets, eight eclogitic garnets and three eclogitic clinopyroxenes. The peridotitic garnets are mostly harzburgitic (seven specimens) with low CaO (from 1.5 to 4.3 wt%), high Cr_2O_3 content (from 8.0 to 18.2 wt%) and a molar Mg# of 85.6 to 88.2. Three peridotitic garnets are lherzolitic with higher CaO (from 5.3 to 5.5 wt%) and lower Cr_2O_3 (from 4.7 to 7.0 wt%) content and a Mg# of 83.8 to 85.3. Eclogitic garnets have a molar Ca# of 5.2 to 37.2 and a Mg# of 49.7 to 79.6, falling mostly in the high-Ca field of Aulbach and Smart (2023), with only two garnet inclusions falling in the high-Mg field.

Eclogitic clinopyroxenes are omphacites with a Mg# of 77.3 to 90.3, and a molar Cr# < 2. Sample ddmi-186a (Diavik mine) shows a very high jadeite component, with Al_2O_3 and Na_2O contents of 17.7 and 5.91 wt%, respectively. This pyroxene also has a relatively low diopside content with CaO and MgO contents of 12.7 and 6.20 wt%, respectively.

Table 1
Craton, kimberlite pipe of origin, paragenesis, N content and its aggregation state, residence temperature, pressure and H_2O content for the diamonds and inclusions studied in this work.

Sample	Craton	Kimberlite Pipe	Suite	N_{tot} (at.ppm)	$\%N_B$	T_{res} (°C)	P_{37} (GPa)	Mineral	H_2O (wt.ppm)
ddmi-8a	Slave	A154-South (Diavik)	H	250	4	1080	5.4	Grt	BD
ddmi-48a	Slave	A154-South (Diavik)	E	165	81	1204	6.3	Cpx	14
ddmi-133b	Slave	A154-South (Diavik)	H	418	0	ND	NA	Grt	BD
ddmi-166c	Slave	A154-South (Diavik)	E	3833	36	1077	5.4	Grt	BD
ddmi-175b	Slave	A154-South (Diavik)	H	294	0	ND	NA	Grt	BD
ddmi-186a	Slave	A154-South (Diavik)	E	822	0	ND	NA	Cpx	289
ddmi-199b	Slave	A154-South (Diavik)	L	994	4	1050	5.2	Grt	BD
ddmi-205b	Slave	A154-South (Diavik)	E	860	0	ND	NA	Grt	BD
ddmi-208b	Slave	A154-South (Diavik)	E	1791	34	1093	5.5	Grt	BD
ddmi-216a	Slave	A154-South (Diavik)	H	219	37	1146	5.9	Grt	BD
GK-13	Slave	Gahcho Kué	L	1277	NA	ND	NA	Grt	BD
GK-19	Slave	Gahcho Kué	E	35	78	1242	6.5	Grt	BD
GK-29	Slave	Gahcho Kué	E	1416	10	1063	5.3	Grt	BD
GK-33	Slave	Gahcho Kué	E	21	NA	ND	NA	Cpx	BD
GK-34B	Slave	Gahcho Kué	H	63	NA	ND	NA	Grt	BD
GK-35	Slave	Gahcho Kué	H	49	1	1085	5.5	Grt	BD
GK-51A	Slave	Gahcho Kué	L	17	1	1109	5.6	Grt	BD
GK-57B	Slave	Gahcho Kué	E	781	7	1068	5.4	Grt	BD
GK-64E	Slave	Gahcho Kué	H	167	99	1294	6.9	Grt	BD
GK-82B	Slave	Gahcho Kué	E	1112	16	1080	5.4	Grt	BD
GK-88A	Slave	Gahcho Kué	E	36	1	1092	5.5	Grt	BD

"H", "E" and "L" refer to the harzburgitic, eclogitic and lherzolitic parageneses, respectively. "Grt" and "Cpx" refer to the minerals garnet and clinopyroxene. "NA" refers to data that were not analyzed/not available, "ND" refers to residence temperatures (T_{res}) that could not be determined either due to N being observed exclusively as A-centers ($\%N_B = 0$), or because the N-aggregation was not measured/reported in the original manuscripts, "BD" indicates values of H_2O content below the detection limit (see text). The T_{res} for the diamonds was calculated assuming a mantle residence time of two billion years using N-aggregation thermochronometry, following Leahy and Taylor (1997). Assuming residence times of one and three billion years results in a differences in the T_{res} of ±20 °C. Pressure was calculated by projecting the T_{res} on a geotherm with a surface heat flow of 37 mW/m^2 (Hasterok and Chapman, 2011). Samples from Diavik were investigated by Donnelly et al. (2007) and those from Gahcho Kué by Siva-Jothy (2020).

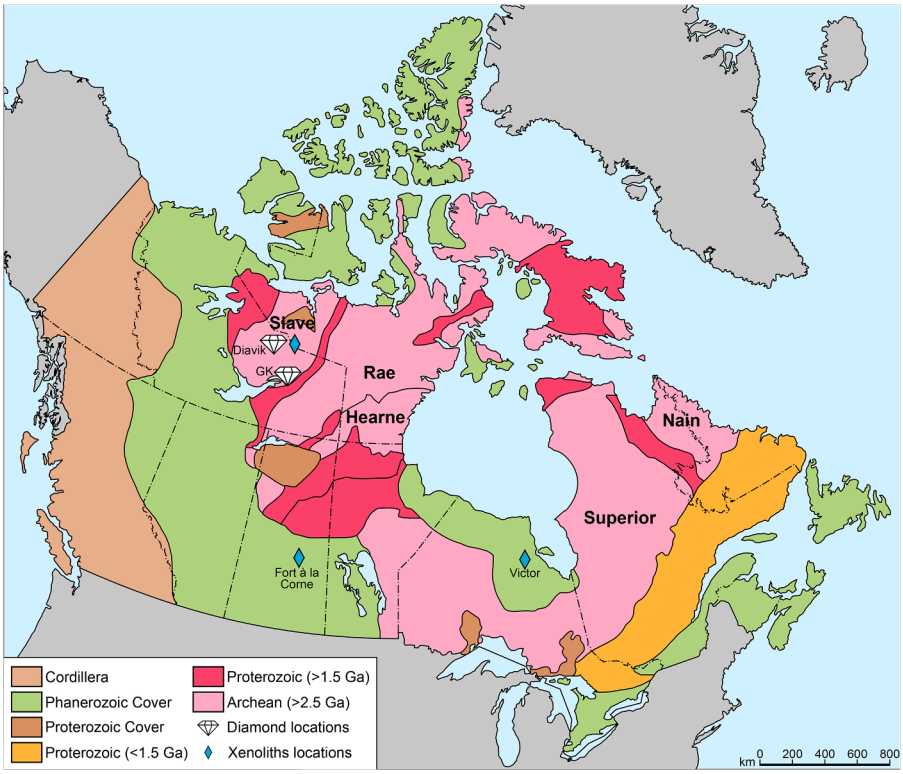


Fig. 1. Geological map of Canada showing the source locality of the diamonds studied in this work. In light blue are the localities of xenoliths from which the H_2O content of minerals has been previously analyzed (Kilgore et al., 2020; Aulbach et al., 2023; Davies et al., 2025; Schmädicke et al., 2025). For the Diavik mine (Slave craton) data from both diamonds and xenoliths are available. Modified after Curtolo et al. (2023).

The other two eclogitic clinopyroxenes have lower jadeite and higher diopside content. Sample ddmi-186a also shows a relatively high concentration of Al in tetrahedral coordination ($^{IV}Al = 2 - Si$) of 0.08 apfu, compared to the other two samples with no tetrahedrally coordinated Al ($^{IV}Al < 0.01$ apfu).

2.2. Fourier-Transform infrared spectroscopy

FTIR spectroscopy was used to measure the H_2O content of the extracted mineral inclusions. Spectra were acquired using a Thermo Scientific Nicolet iN10 infrared microscope equipped with an EverGlo air-cooled infrared source, a KBr beamsplitter and a liquid nitrogen cooled MCT detector (Department of Geosciences, University of Padova). Both background and inclusion spectra were collected though a BaF_2 plate, accumulating 64 scans with a total scan time of 22 s and a spectral resolution of 4 cm^{-1}. Prior to measuring, the inclusions were manually cleaned several times with ethanol; however, due to their small size, signal due to contamination from organic material (most likely epoxy resin from previous mounting for polishing and EPMA analysis) remained visible at ~2800–2900 cm^{-1} (see Fig. 2).

Inclusions were measured using unpolarized radiation on randomly oriented grains, the uncertainty for this type of measurement is expected to be ~30% (Curtolo et al., 2025a). If possible, more than one orientation was measured for each inclusion, and the mean H_2O content was calculated from spectra recorded for each distinct orientation. Moreover, sample ddmi-186a, which showed the strongest OH absorption bands, was measured using polarized radiation in two random orientations at the Bayerisches Geoinstitut (Universität Bayreuth, Bayreuth, Germany). Baseline correction was done using cubic spline functions. The H_2O content of the minerals was calculated using the integrated absorbance of the signal associated with OH stretching in the 3000 to 3700 cm^{-1} region and employing the absorption coefficients of Bell et al. (1995) for garnet and Koch-Müller et al. (2007) for clinopyroxenes. The absorption coefficient of Koch-Müller et al. (2007) was chosen because of the similar composition of the clinopyroxene in this study with those used for the calibration, as well as the fact that they exhibit H mainly in the M-site as opposed to the T-site.

The thickness of the clinopyroxene inclusions, which is required for calculation of H_2O contents from FTIR spectra, was measured with an Olympus LEXT OLS4000 laser scanning confocal microscope equipped with a 405 nm laser diode light source and a high sensitivity photomultiplier (Department of Geosciences, University of Padova). Three-dimensional models of each inclusion were produced with a resolution < 1 μm and the thickness of each inclusion was calculated as the average thickness of several (> 5) cross-sections measured on the 3D model in the direction of propagation of the radiation. The thickness of the garnet inclusions was measured under a Leica optical microscope with an estimated accuracy of $\pm$ 10 μm. All thicknesses are reported in Table S2.

3. Results

3.1. H_2O content of mineral inclusions in diamonds

All garnet inclusions have H_2O contents below the FTIR detection limit (Table 1, Fig. 2a,b), in agreement with similar studies on garnet inclusions in diamond (Matsyuk et al., 1998; Novella et al., 2015; Taylor et al., 2016; Curtolo et al., 2025a). Two of the three clinopyroxene inclusions (ddmi-48a and ddmi-186a) show absorbance in the OH stretching region. The absorption bands belong mainly to group 1 (3345–3465 cm^{-1}) with a less intense group 2 (3500–3540 cm^{-1}) band observed only in sample ddmi-186a (Fig. 2c, Fig. S1). Group 1 bands are associated with H incorporation related to vacancies in the M2 site (Koch-Müller et al., 2004). The two clinopyroxenes showing OH-related absorption bands have H_2O contents of 14 and 289 wt.ppm. The third investigated clinopyroxene shows no absorption bands in this region and therefore has an H_2O content below the FTIR detection limit (Table 1,

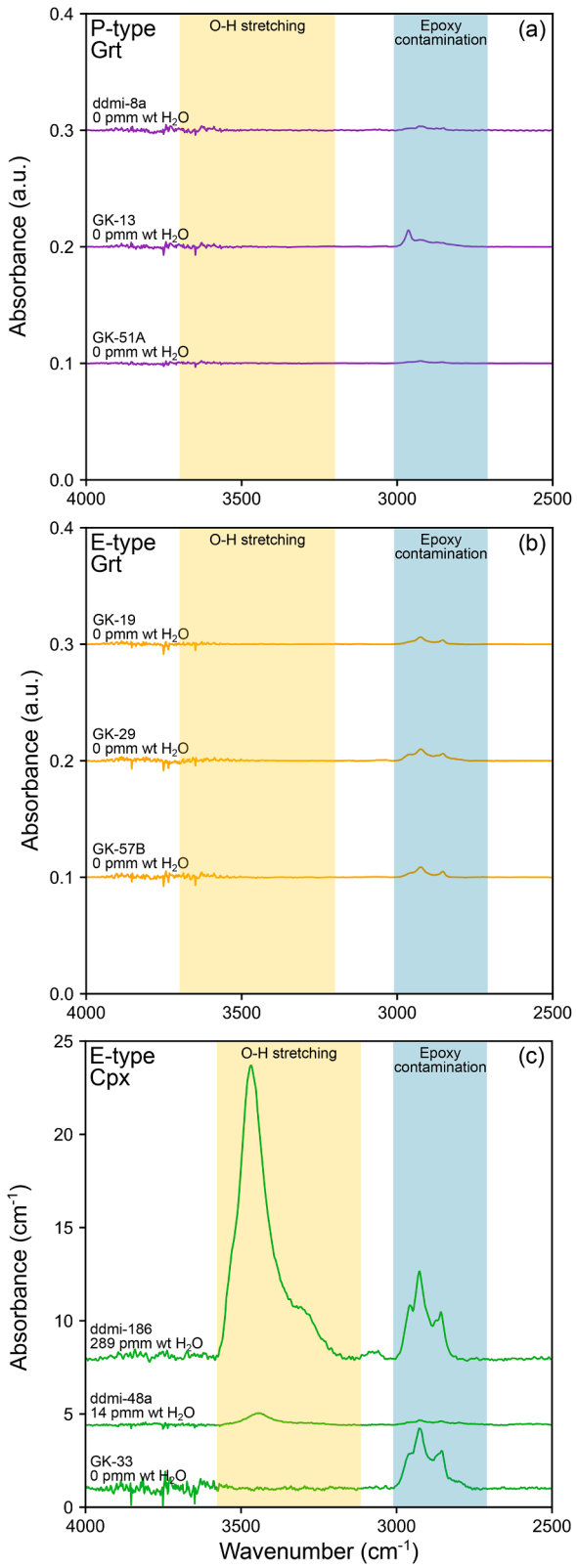


Fig. 2. Representative FTIR spectra of (a) P-type (peridotitic), (b) E-type (eclogitic) garnets and (c) E-type clinopyroxenes analyzed in this study. The area highlighted in light blue is the spectral region showing signal due to contamination from epoxy resin. The area highlighted in yellow shows the principal OH-stretching region. Noise around 3700 cm^{-1} is due to atmospheric water. The absorbance in (a) and (b) is expressed in arbitrary units and in (c) it is normalized to a sample thickness of 1 cm. All the spectra are offset for clarity.

Fig. 2c). These values are in agreement with those previously reported for diamond-hosted eclogitic clinopyroxene inclusions (Taylor et al., 2016; Curtolo et al., 2025a).

3.2. Thermodynamic modeling of COH speciation

To investigate the H_2O content of diamond-forming fluids in relation with the H_2O content of diamond-hosted mineral inclusions studied here, a new thermodynamic model was developed to calculate the COH speciation of a fluid along geotherms appropriate for the cratonic lithosphere (i.e., with a surface heat flow of 35, 37 and 40 mW/m^2, Hasterok and Chapman 2011). The model was constructed assuming C saturation (i.e., fluid in equilibrium with graphite/diamond) and details are reported in Appendix I.

Results from this model are reported in Fig. 3, and show that a COH fluid in equilibrium with graphite at 2 GPa will be composed almost exclusively of H_2O (97 to 99 mol% H_2O depending on the geotherm) with minimal amounts of CO_2 or CH_4 (< 1 mol% CO_2 and 1 mol% CH_4 along a 35 mW/m^2 geotherm and 3 mol% CO_2 and < 1 mol% CH_4 along a 40 mW/m^2 geotherm). As pressure and temperature increase, and fO_2 decreases, the amount of H_2O and CO_2 decreases while the CH_4 concentration increases. At the phase boundary between graphite and diamond, the fluid is primarily composed of H_2O and CH_4 (92 to 90 mol% and 7 to 8 mol% respectively, depending on the geotherm) with up to 1 mol% H_2 along the 40 mW/m^2 geotherm. At ~6 GPa (the pressure mode for diamond formation, see Nimis, 2022), the fluid will be composed of 61, 66 and 71 mol% H_2O (equivalent to 65.1, 70.0 and 75.6 wt%) along the 35, 37 and 40 mW/m^2 geotherms, respectively. Along with H_2O, at these pressure and temperature conditions, the fluid is also composed of 36 to 25 mol% CH_4 and 2 to 4 mol% H_2. Increasing pressure from this point, more CH_4 and H_2 will stabilize at the expense of H_2O until, eventually, H_2O will become a negligible component of the fluid.

These results contrast with those of previous models (see e.g., Frost and McCammon, 2008 and Shirey et al. 2013) which predicted the fluid, at diamond-forming conditions, to be at the "water maximum" (90–99 mol% H_2O, see Shirey et al., 2019). This is most likely due to previous models being solved accounting for the pressure-tempereature profile of a convective adiabat instead of a conductive geotherm (Frost and McCammon, 2008) or fixing pressure and temperature to a single value and varying fO_2 (Shirey et al., 2013). The results of this model therefore suggest that diamond-forming COH fluid in the cratonic lithosphere, will have an H_2O content substantially lower than previously suggested, and $a_{H_2O} < 1$.

4. Discussions

4.1. Mineral H_2O contents and major element composition

To discuss possible correlations between the H_2O content and composition of the studied samples, the inclusions in diamonds were compared with compositional data available in the literature for minerals from Canadian xenoliths with a known H_2O content (Kilgore et al., 2020; Aulbach et al., 2023; Davies et al., 2025; Schmädicke et al., 2025).

Pressure estimates for samples investigated in this study show that they originated between 5 and 7 GPa, in agreement with previously suggested diamond-formation depths (see e.g., Nimis, 2022) and on the deeper end of the range for xenoliths from the Canadian lithosphere (Fig. 4). The only exception being peridotitic garnets, where the data from inclusions in this study almost perfectly overlap with the range of pressures exhibited by garnets from peridotitic xenoliths from Diavik (Fig. 4c).

Comparison with data from xenoliths from the Canadian cratons shows that, regardless of mineral and paragenesis, diamond-hosted mineral inclusions show H_2O contents lower than those measured in the same minerals from xenoliths for comparable depths in the lithosphere (Fig. 4, Fig S2). This was previously recognized by Peslier et al.

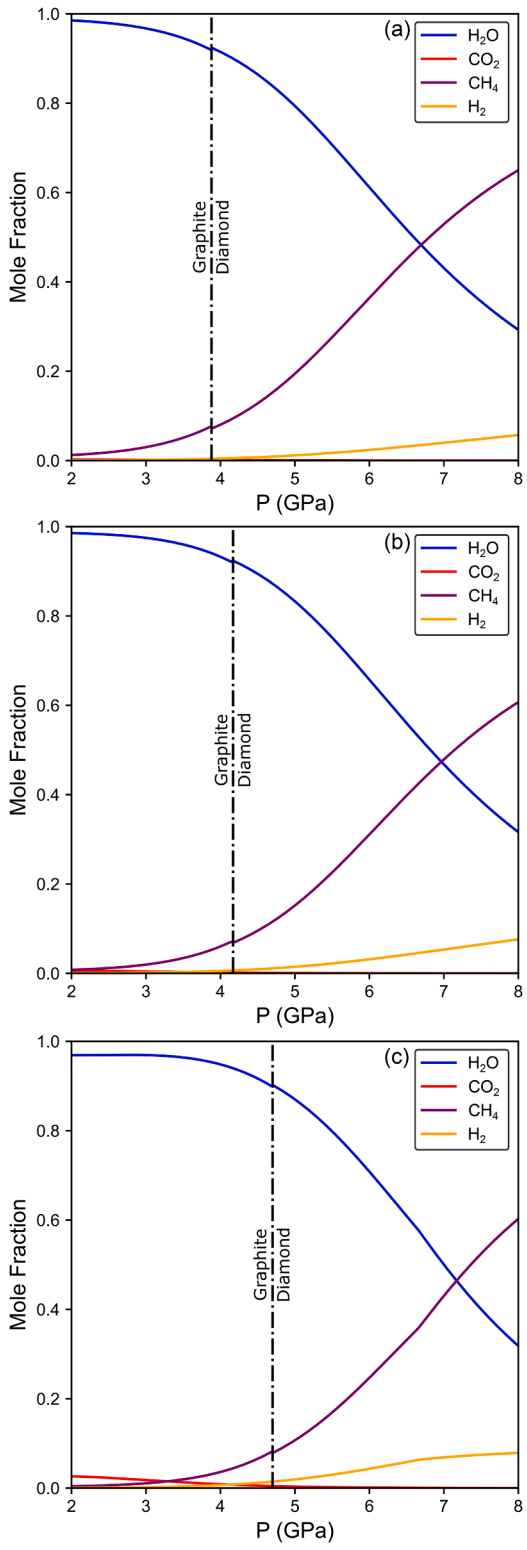


Fig. 3. Thermodynamic model of COH fluid speciation along a 35 (a), 37 (b) and 40 (c) mW/m^2 conductive geotherm. Further details regarding the model are reported in Appendix I.

(2017), who attributed this difference to metasomatic alteration of the xenoliths, and by Curtolo et al. (2025a), who attributed this difference to low H_2O activity in the diamond forming fluid. Davies et al. (2025) also invoked low H_2O activity to explain the lower H_2O content of a diamondiferous eclogitic xenolith compared to diamond-free xenoliths from the same locality (Fort à la Corne, Canada).

No trend is observed between the pressure and the H_2O content of NAMs, neither for minerals in xenoliths nor for diamond-hosted inclusions. A weak trend of decreasing H_2O content with increasing pressure might be suggested for eclogitic clinopyroxenes, however such a trend is absent when considering the individual localities by themselves. This implies that no correlation exists between the pressure and the H_2O content of these minerals.

There is a general overlap in the major element composition of garnets from this study and from Canadian xenoliths (Fig. S3). The only difference being peridotitic garnets, which are dominated by the harzburgitic paragenesis in this study, while no harzburgitic garnets from Canadian xenoliths have been studied for their H_2O content (Fig. S3a). This is also reflected in the Mg# and Ca# of peridotitic garnets (Fig. S3b), where samples from this study mostly show higher Mg# and lower Ca# (characteristic of harzburgitic garnets) compared to samples from Canadian xenoliths.

Metasomatic alteration of eclogitic garnets, due to interaction with kimberlite-like melts, is thought to be associated with an increase in Mg# and a decrease in Ca# (e.g., Aulbach et al., 2024). This trend is observed in samples (both inclusions and xenoliths) from the Gahcho Kué ($r = -0.99$, $p < 0.05$, where r refers to Pearson's correlation coefficient and p is the p-value obtained for a two-tailed test), and Victor ($r = -0.87$, $p < 0.05$) kimberlites, but not in those from Diavik and Fort à la Corne ($p >> 0.05$; Fig S3c). Despite the observed negative correlation between Mg# and Ca#, no statistically significant correlation between H_2O content and Mg# or Ca# was observed, neither by considering all localities together nor separately ($p >> 0.5$; Fig. S4).

Metasomatic alteration of peridotitic garnet is expected to result in a higher Ca# and lower Mg# (O'Reilly and Griffin, 2013). This trend is observed in garnets from Gahcho Kué ($r = -0.89$, $p < 0.05$) but it is not observed in those from Diavik ($p > 0.05$, Fig. S3b). The H_2O content of peridotitic garnets shows no significant correlation ($p > 0.05$) with Mg# and Ca#, either for diamond-hosted inclusions or for minerals in xenoliths (Fig. S5a,b). Metasomatism of peridotitic garnet is also thought to be associated with an increase in TiO_2 content (Peslier et al., 2017) but no significant correlation is observed between the TiO_2 and H_2O content of the peridotitic garnets ($p > 0.05$; Fig. S5c).

The major element composition of clinopyroxenes in this study also closely overlaps with that of eclogitic clinopyroxenes from Canadian xenoliths (Fig. S6). The only outlier appears to be sample ddmi-186a from Diavik (Slave craton), which has a low Mg and Ca content (low diopside content) compared to all the other clinopyroxenes (Fig. S6b) and at the same time shows a very high Al content falling outside the positive Na-Al correlation representative of the jadeite component (Fig. S6c). This sample in fact shows the highest amount of Al in tetrahedral coordination (^{IV}Al) out of all the samples considered here (Fig. 5c).

Ultramafic metasomatism of eclogitic clinopyroxenes is thought to be associated with an increase in Mg# and a decrease in the jadeite component (Aulbach et al., 2024). However, no correlation is observed between the H_2O content and Mg#, Na or Al ($p > 0.05$; Fig. 5a,b,d). A correlation in H_2O vs. Al ($r = 0.86$, $p < 0.05$) and H_2O vs. Na ($r = 0.88$, $p < 0.05$) is observed in clinopyroxenes from xenoliths from the Victor mine. However, the samples show an increase in H_2O content with increasing jadeite component, the inverse of what is expected for metasomatic overprinting, but in agreement with what is expected for melt extraction. Tetrahedrally-coordinated Al in clinopyroxene is well-known to promote H_2O incorporation following the coupled substitution $Si^{4+} = {}^{IV}Al^{3+} + H^+$ (see, e.g., O'Leary et al., 2010). However, no correlation between ^{IV}Al and the H_2O content is observed in the present dataset ($p > 0.05$; Fig. 5c). This may reflect an operative substitution mechanism in which ^{IV}Al is not charge-balanced by H^+ such as the Tschermak substitution ($^{VI}M^{2+} + {}^{IV}Si^{4+} = {}^{VI}Al^{3+} + {}^{IV}Al^{3+}$). In this case, incorporation of ^{IV}Al is not accompanied by H incorporation thus weakening or obscuring the correlation between ^{IV}Al and H_2O content.

The overall lack of correlation between metasomatic indicators

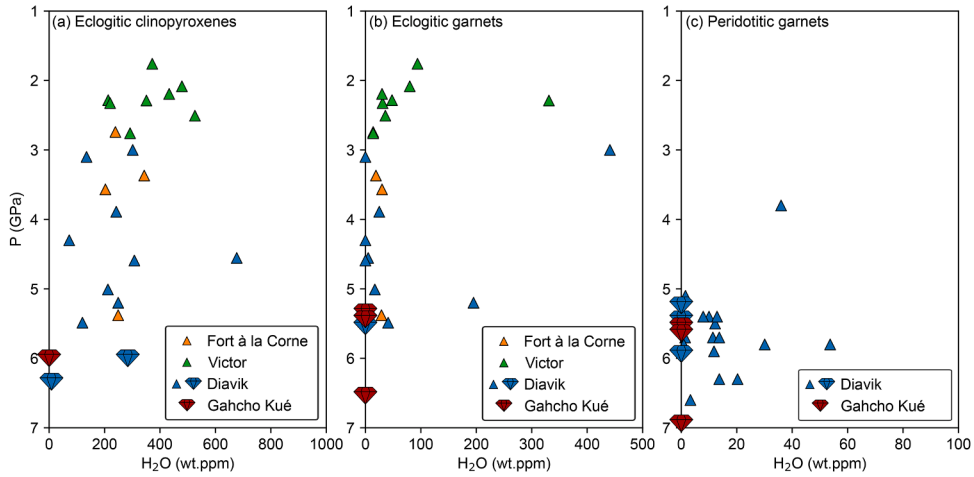


Fig. 4. H_2O content plotted as a function of pressure (in GPa, pressure increasing downwards) for all samples in this study (diamond symbols) as well as for minerals from Canadian xenoliths (triangle symbol). Pressures used for the diamond-hosted inclusions are those reported in Table 1. For two of the three diamond-hosted clinopyroxene inclusions (samples ddmi-186a and GK33) pressure could not be calculated, therefore they have been plotted at a pressure of 6 GPa, corresponding to the global mode of diamond formation (Nimis, 2022). Data for xenoliths are from Kilgore et al. (2020), Aulbach et al. (2023), Davies et al. (2025) and Schmädicke et al. (2025), pressures for these data were either reported in the original manuscript or have been calculated using the geobarometer of Nimis and Taylor (2000) for peridotitic samples and that of Beyer et al. (2015) for eclogitic samples.

(major elements) and the H_2O content in the samples studied here may suggest a decoupling between H_2O and these elements, as previously suggested by Aulbach et al. (2024) for eclogitic clinopyroxenes. Alternatively, the metasomatic history of the samples considered in this study may be complex, where multiple episodes of enrichment and depletion of various elements due to different metasomatic agents may have eliminated any expected trend.

4.2. The H_2O content of diamond-forming fluids

According to Weiss et al. (2022), diamond-forming fluids are either low-density fluids, such as COH supercritical fluids, or high-density fluids, such as melts of various compositions (e.g., silicic, carbonatitic, metallic). The thermodynamic model described in Section 3.2. calculates the speciation of a pure, low-density COH fluid, and shows that depending on the pressure, temperature, and fO_2 conditions the composition of the fluid at C saturation can range from almost pure H_2O to $CH_4 + H_2$ (+ very low amounts of H_2O). However, pure COH fluids are unlikely to occur in the deep mantle as the solubility of silicates in such fluids increases with pressure and temperature (up to 70 wt% at 8 GPa, Mibe et al., 2002). Moreover, at diamond-forming conditions, both the peridotite-H_2O and basalt-H_2O systems surpass their second critical endpoint (Mibe et al., 2007;2011), resulting in complete miscibility between low-density fluids and silicate melts. The pure COH fluid modelled above should therefore be considered as a maximum H_2O endmember where in reality, COH fluids with a high dissolved solute content or silicate melts likely have an even lower H_2O content than predicted here.

Even before the miscibility gap between aqueous fluids and silicate melts closes, high-density fluids can have highly variable H_2O contents. Experimental works from Kessel et al. (2015) show that fluids in equilibrium with peridotite at 4–6 GPa and 900–1200 °C have H_2O contents ranging from 64.4 wt% at low temperatures to 24.1 wt% at high temperatures. Fluids with high H_2O contents (~60 wt%) are likely to form from dehydration reactions occurring in subducting slabs, where temperatures are such that melting does not occur. At higher temperatures, the hydrous solidus of mantle rocks would be exceeded resulting in a H_2O-bearing silicate melt. In the mantle, melt fractions are expected to be small, and according to experimental works that synthesized H_2O-bearing low-degree melts in equilibrium with a mantle peridotite at 6 GPa and 1400 °C (Novella and Frost, 2014), their expected H_2O content is ~11 wt%. The H_2O content of such melts will change based on the pressure and temperature conditions of melting, the partition coefficients and the bulk H_2O content of the mantle rocks (Kovács et al., 2012). If the temperature is higher than the solidus temperature, more melt will be produced with relatively lower H_2O content. On the other hand, if the mineral/melt H_2O partition coefficients are decreased (e.g., due to CO_2 in the system; see Sokol et al., 2013; Curtolo et al., 2025b), the melt in equilibrium with the rock will have relatively higher H_2O content. Regardless of the uncertainties in the estimated H_2O content of a low-degree melt in the mantle, it is unlikely that H_2O content will vary significantly from the 11 wt% predicted by Novella and Frost (2014) at similar pressure conditions. In fact, this value is very close to the H_2O content of silicic fluid inclusions (9.8 wt%) in fibrous diamonds calculated by Weiss et al. (2022). Apart from silicic fluids, Weiss et al. (2022) recognized other types of fluid inclusions in fibrous diamonds, namely saline and carbonatitic compositions. The former consists of brines with high H_2O and CO_2 concentrations (21.3 and 10.7 wt%, respectively; see Weiss et al., 2022) that may form due to immiscibility between brines and silicate melts (Weiss et al., 2022) or as a result of dissolution of salts and other rock-forming elements in COH-bearing aqueous fluids. Carbonatitic fluid inclusions (low- and high-Mg carbonatitic) resemble carbonatitic melts with high CO_2 contents (26.1–31.7 wt%) and lower H_2O contents compared to saline fluids (10.7–7.6 wt%, Weiss et al., 2022).

According to this experimental and natural evidence, it is reasonable to assume that diamonds do not form from pure aqueous fluids, but instead from a range of high-density fluids (melts and brines) with volatile contents that are < 40 wt%.

4.3. H_2O in inclusions in equilibrium with diamond-forming fluids

To evaluate the expected H_2O content of diamond-hosted mineral inclusions in equilibrium with a diamond-forming fluid, a thermodynamic water incorporation model was developed which follows the equation:

$$c_{H_2O} = A f H_2O^n \exp\left(-\frac{\Delta H^{1bar} + \Delta VP}{RT}\right)$$

where c_{H_2O} is the concentration of H_2O in the mineral, A is an empirical parameter, fH$_2$O is the fugacity of H_2O, n is an exponent that depends on the stoichiometry of the H incorporation reaction, P is the pressure and

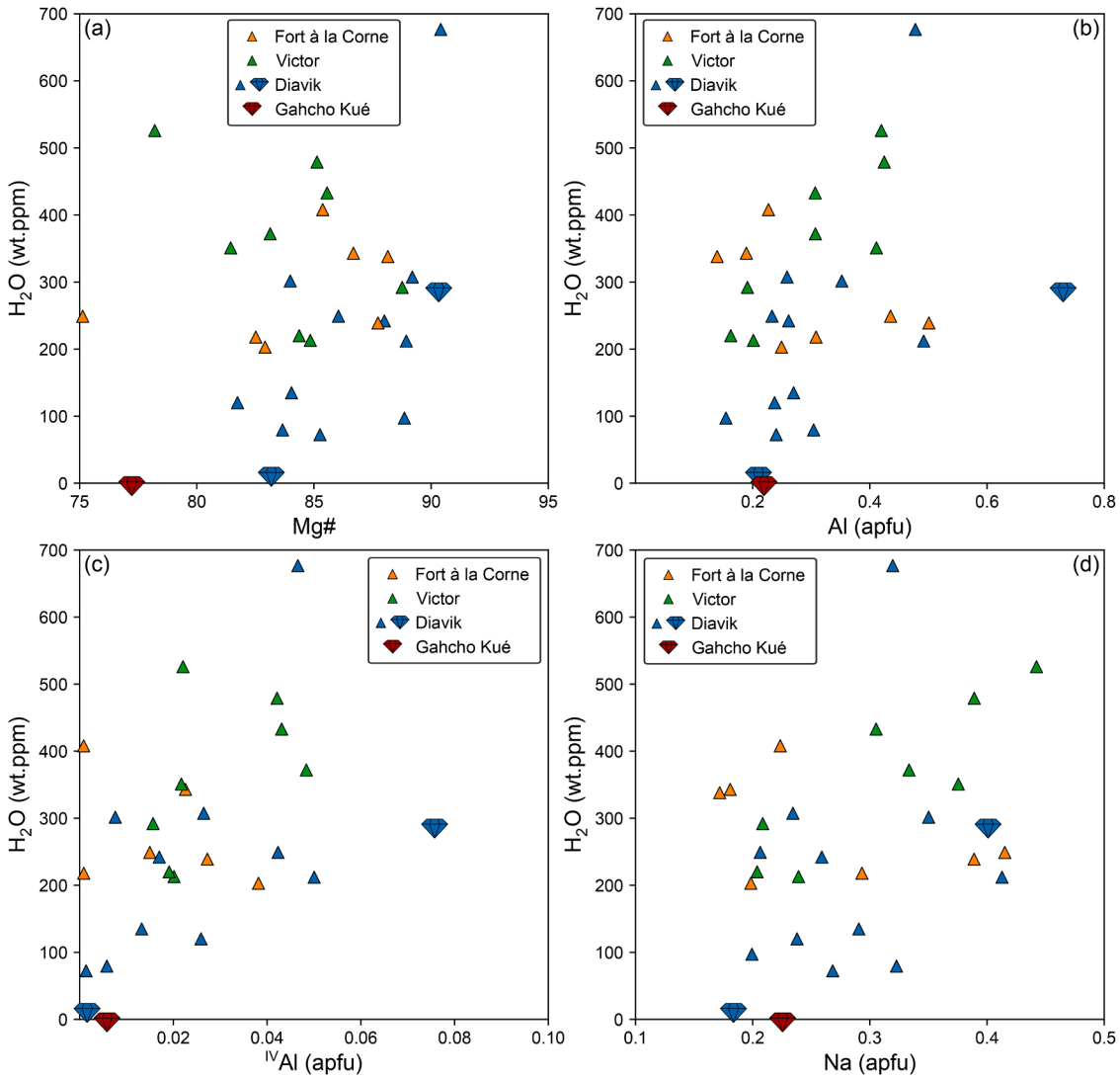


Fig. 5. H_2O content plotted as a function of the major element composition of eclogitic clinopyroxenes from xenoliths (triangle symbols) and from diamonds (diamond symbols). Apfu: atoms per formula unit.

ΔH^{1bar} and ΔV are the enthalpy and volume change of the reaction (Keppler and Bolfan-Casanova, 2006). This model allows calculation of the H_2O content of a mineral at any pressure, temperature and fH_2O condition, provided that the necessary parameters are known from previous experimental calibrations.

For olivine, the calibration of Kohlstedt et al. (1996) was employed, which describes water incorporation related to a divalent cation vacancy (i.e., $Me^{2+} = 2OH^{-}$; $n = 1$). For orthopyroxene the calibration of Mierdel and Keppler (2004) was used, which was obtained from experiments on pure enstatite and involves H_2O incorporation related to vacancies of divalent cations. For peridotitic clinopyroxenes, the calibration of Gavrilenko (2008) for pure diopside ($n = 1$) was used in combination with that of Bromiley et al. (2004) for Cr-bearing diopside ($n = 0.5$). This accounts for water incorporation associated with both divalent cation vacancies at the M2-site and coupled substitutions either at the M1- or T-site (e.g., $^{T}Si^{4+} = {}^{T}Al^{3+} + H^{+}$ or $^{M1}Fe^{3+} = {}^{M1}Fe^{2+} + H^{+}$), which explain most of the bands observed in the spectra of peridotitic clinopyroxenes (see Balan et al., 2020). For eclogitic clinopyroxene, on the other hand, the calibration of Gavrilenko (2008) was combined with that of Bromiley and Keppler (2004) for jadeite ($n = 0.5$). This, on a first approximation, reproduces natural eclogitic clinopyroxenes which can be thought of as a solid solution of diopside and jadeite. For garnet, the calibration of Lu and Keppler (1997) was used. This calibration was based on experiments on a natural pyrope from Dora Maira where water incorporation was related to B and Li impurities substituting for Si and Mg ($n = 0.5$). This is unlikely to be representative of natural mantle garnets, nevertheless it remains the only currently available calibration for garnet.

Calculations were done for NAMs in equilibrium with a pure COH fluid along a 37 mW/m^2 geotherm following the results of the model described in Section 3.2 and assuming ideal mixing (the fugacity of H_2O in the fluid was therefore given by $fH_2O = X_{H_2O}\Phi_{H_2O}P$, where Φ_{H_2O} is the fugacity coefficient of pure H_2O and X_{H_2O} is the calculated molar fraction of H_2O in the mixture). The results of these calculations are shown in Fig. 6a.

Despite its advantages, this model also has some shortcomings. Firstly, it is based on equilibration experiments performed on pre-existing crystals which impose a point-defect structure that is decorated by H, and may therefore not be representative of how H_2O incorporation really occurs in natural environments (see Tollan et al., 2018). Secondly, not all calibrations obtained ΔH^{1bar} (only the models for pure enstatite and diopside) and the available calibrations cover only specific incorporation reactions, which may not be representative of all reactions involved in a realistic mantle environment, where minor and trace elements may play an important role in H_2O incorporation in NAMs. The purpose of these calculations, however, is not to rigorously

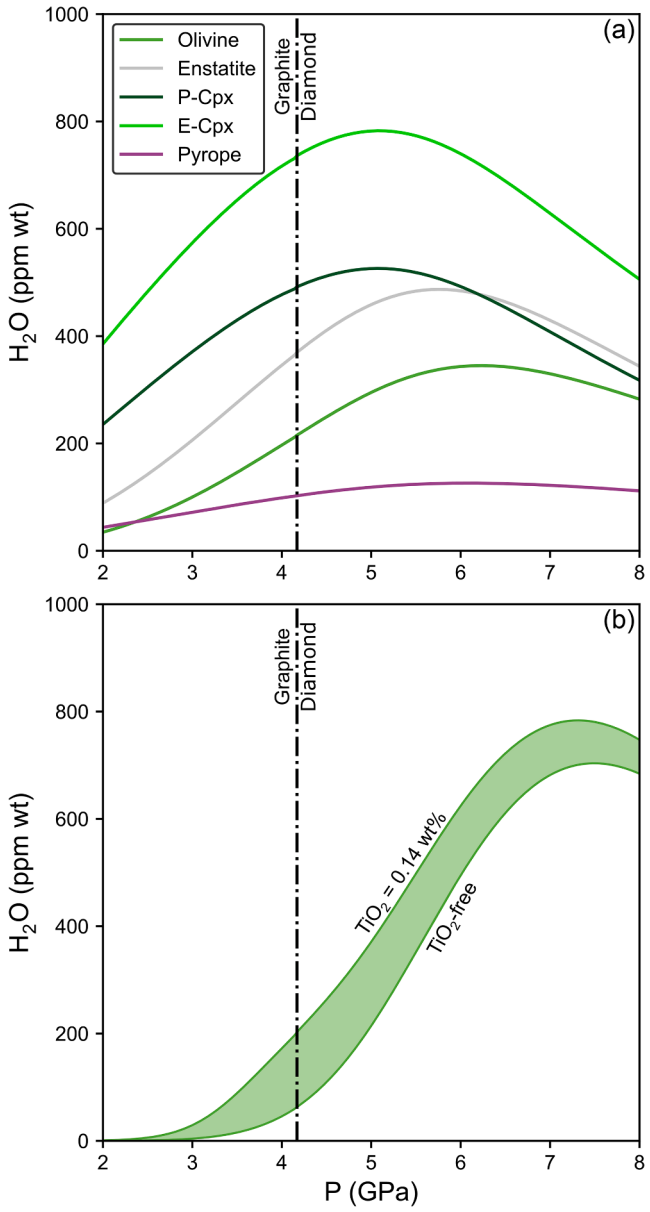


Fig. 6. Calculated H_2O content of NAMs in equilibrium with a pure COH fluid along a 37 mW/m^2 geotherm. (a) Results obtained using the calibration of Kohlstedt et al. (1996), Mierdel and Keppler (2004), Gavrilenko (2008), Bromiley et al. (2004), Bromiley and Keppler (2004) and Lu and Keppler (1997). (b) Results obtained using the calibration of Padrón-Navarta and Hermann (2017) for TiO_2-free olivines and for olivines with a TiO_2 content of 0.14 wt% (the highest value reported for diamond-hosted olivine inclusions; Stachel et al., 2022a).

reproduce the absolute H_2O contents of natural mantle NAMs, but rather to illustrate the influence of pressure, temperature and fH_2O on water incorporation. Differences between calculated and observed H_2O contents may reflect variations in defect populations, trace-element chemistry and fluid composition that are not explicitly included in the model.

The results of this model are compared with the calculated H_2O contents in olivine obtained using the model of Padrón-Navarta and Hermann (2017), which explicitly treats H_2O incorporation in olivine related to Si vacancies and Ti-clinohumite defects as a function of pressure, temperature and TiO_2 concentration. For this model, H_2O contents for systems with $a_{H_2O} < 1$ (like the COH fluid used for the model) are calculated assuming ideal mixing ($a_{H_2O} = X_{H_2O}$) and considering the stoichiometry of the reaction (i.e., $c_{H_2O} \propto X^2_{H_2O}$ for Si vacancies and $c_{H_2O} \propto X_{H_2O}$ for the Ti-clinohumite defect, Tollan et al., 2017). At present, no similar calibrations are available for other minerals, so this model can be applied only to olivine, and the results are shown in Fig. 6b

Comparison of these two approaches reveals how sensitive the H_2O content of olivine is based on the assumed incorporation mechanism and the chosen calibration. The calibration of Kohlstedt et al. (1996) predicts higher H_2O contents at low pressure and temperature conditions and lower H_2O contents at high pressures and temperatures compared to the model of Padrón-Navarta and Hermann (2017). This reinforces the fact that an accurate calculation of the H_2O content of NAMs requires a rigorous description of all the incorporation mechanisms involved and their thermodynamic properties.

Regardless of the absolute H_2O content, both the models predict H_2O concentrations which are markedly higher than what is observed in NAM inclusions in diamonds, confirming that pure COH fluids are unlikely to be representative of diamond-forming fluids in the mantle. Instead, COH-bearing brines/melts, as observed by Weiss et al. (2022), are more likely in diamond-forming environments. In these kind of fluids, COH species comprise at most ~40 wt% of the total composition, this reduces the activity of H_2O at all pressures, temperatures and fO_2, and will therefore lead to a lower predicted H_2O content of NAMs in equilibrium with such fluids.

In Fig. 7 the dependence of the H_2O content of olivine on X_{H_2O} in a fluid is illustrated according to the incorporation model of Kohlstedt et al. (1996) and Padrón-Navarta and Hermann (2017). The inferred X_{H_2O} necessary to produce the H_2O content measured in diamond-hosted olivine inclusions varies substantially depending on the assumed H incorporation mechanism, with the highest X_{H_2O} obtained for the case where all H incorporation is related to Si (T-site) vacancies. Even when the uncertainties inherent to this kind of model (e.g., the operative H incorporation mechanisms, and the precise pressures, temperatures, fO_2 and compositions) are accounted for, the observed H_2O contents of olivine require fluids with H_2O activities far below those expected for a pure COH fluid. These considerations about different H incorporation mechanisms and their influence on the H_2O content can be extended to other NAMs. For example, if H incorporation in garnet occurs mainly as hydrogarnet-type substitution (as suggested in many works e.g., Geiger and Rossman 2018;2020a, b; Reynes et al., 2020) then $c_{H_2O} \propto X^2_{H_2O}$ resulting in a rapid decrease in the concentration of H_2O in garnet as the activity of H_2O decreases. This may explain the often very low H_2O contents observed in diamond-hosted garnet inclusions and in mantle garnets in general. Conversely, in clinopyroxenes H may be incorporated through a combination of coupled substitutions involving single H atoms and divalent cation vacancies. In these cases, $c_{H_2O} \propto X^{0.5}_{H_2O}$ and $c_{H_2O} \propto X_{H_2O}$ (Balan et al., 2020) and thus clinopyroxenes would retain measurable H_2O contents even in equilibrium with fluids characterized by low H_2O activities, in agreement with the relatively high average H_2O content of diamond-hosted clinopyroxene inclusions.

4.4. The nature of diamond-forming fluids in the lithospheric mantle

Experimental work (see Sokol and Pal'yanov 2007; Luth et al., 2022) shows that the most effective diamond-forming medium is a H_2O-rich COH fluid. However, as discussed previously, at pressure and temperature conditions relevant to diamond formation, a pure COH-fluid cannot exist. Moreover, it has been shown that mantle peridotites are very poor sinks/sources of O_2, meaning that formation of diamond by oxidation of CH_4 (or reduction of CO_2) in a fluid is unlikely to produce significant amounts of diamonds, unless a small amount of fluid interacts with a large region of the mantle (Luth and Stachel, 2014). Alternatively, isochemical precipitation of diamond from COH fluids containing both CO_2 and CH_4 has been proposed and does not require changes in the redox state of the mantle (Luth and Stachel, 2014). However, as shown in the thermodynamic model above (Fig. 3), at the pressure, temperature, and

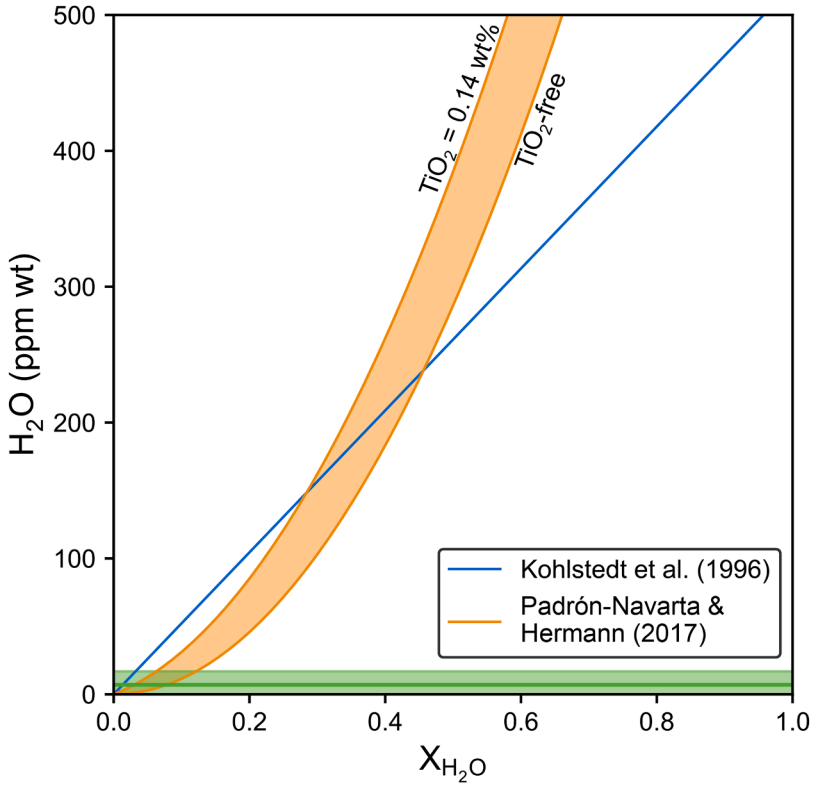


Fig. 7. Calculated H_2O content in olivine as a function of the molar fraction of H_2O in a fluid (assuming ideal mixing, $a_{H_2O} = X_{H_2O}$) at a pressure of 6 GPa along a 37 mW/m^2 geotherm, using the incorporation models of Kohlstedt et al. (1996) in blue and of Padrón-Navarta and Hermann (2017) in orange. The green line shows the average H_2O content measured in diamond-hosted olivine inclusions and the green shaded area represents the standard deviation of the average.

fO_2 conditions of the lithospheric mantle, CH_4 is not in equilibrium with oxidized C species, and thus isochemical precipitation of diamond is unlikely to occur.

Other types of media from which lithospheric diamonds can crystallize are carbonatitic and hydrous-carbonated silicate melts (Luth et al., 2022). Both carbonatitic and hydrous-carbonated silicate melts have been recognized as possible parental fluids involved in the formation of fibrous diamonds (Weiss et al., 2022) and therefore may also be good candidates for gem-quality lithospheric diamond formation. Carbonatitic melts have very low solidus temperatures (Litasov et al., 2013) and extremely low viscosities (Dobson et al., 1996). This allows percolation into cold cratonic lithospheric substrates without freezing, promoting diamond formation if such melts are saturated in C-species (and provided the P, T and fO_2 conditions are compatible with diamond stability). The low H_2O activity in carbonatitic melts (inferred by their high H_2O solubility) agrees with the relatively low H_2O contents observed in most diamond-hosted mineral inclusions (see e.g., Curtolo et al., 2025a and references therein).

Hydrous-carbonated silicate melts can also precipitate diamonds in the lithosphere, albeit likely less efficiently than carbonatitic melts and H_2O—CO_2 fluids (see e.g., Fagan and Luth, 2011; Luth et al., 2022). Due to the solidus-lowering effect of H_2O and CO_2 (see e.g., Dasgupta, 2018; Curtolo et al., 2025b), it is likely that such melts can percolate through the lithospheric mantle without freezing completely. In this regard, a carbonated silicate melt can form in the convective asthenosphere by melting of adiabatically upwelling mantle, it can percolate upwards to the progressively lower pressure and temperature environments in the lithosphere. During percolation and pressure decrease, the solubility of C in such silicate melts decreases (see e.g., Ni and Keppler, 2013) leading to oversaturation in C-species and subsequent diamond precipitation. Here, diamond crystallization could occur without the need for redox reactions involving the surrounding mantle. Two possible diamond-forming reactions are:

$$4OH^- + CO_2 = C + 2H_2O + 4O^0$$

$$CH_4 + 4O^0 = C + 4OH^-$$

where O^0 indicates a bridging oxygen (i.e., oxygen shared by two tetrahedral units). The C, O and H species involved in these reactions are all observed in volatile bearing melts (Stolper, 1982; Mysen, 2012) and allow diamond to precipitate from the melt without oxygen exchange with the surrounding mantle. Instead, these reactions would only cause changes in the polymeric structure of the melt (e.g., the conversion of bridging to non-bridging oxygens and *vice-versa*). It is important to note that these reactions are only theoretical, as they have never been observed, and no information is available on their ΔG and/or K.

Based on the above discussions, it can be concluded that the most efficient diamond-forming medium in the mantle consists of carbonatitic melts in which C-species oversaturation promotes diamond precipitation. These melts can be associated with diamond formation in peridotitic substrates as their low H_2O activities may explain the low H_2O content observed in peridotitic inclusions. Formation of eclogitic diamonds from both carbonatitic and hydrous-carbonated silicate melts may explain the large variation in H_2O contents observed in eclogitic mineral inclusions. This is because the H_2O partition coefficient between minerals and silicate melts decreases with increasing CO_2 content in the melt (see Sokol et al., 2013; Curtolo et al., 2025b) as a consequence of decreasing H_2O activity. It follows that the lowest H_2O contents observed in eclogitic mineral inclusions are likely associated with carbonatitic melts (with low H_2O activity). High H_2O contents may be associated with hydrous-carbonated silicate melts with low C contents and intermediate H_2O contents, a potential result of different H and C proportions in the melt. Furthermore, the relatively low H_2O contents hypothesized here for diamond-forming fluids may also explain the lack of FTIR-detectable water in fluid films observed around mineral

inclusions in diamond (Nimis et al., 2016). If, as hypothesized, these rims represent the remnants of the diamond-forming fluid (Nimis et al., 2016), their low H_2O content, coupled with their low thickness (~1 μm, see Nimis et al. 2016; Curtolo et al., 2025a) would result in an extremely low absorbance below the FTIR detection limit.

5. Conclusions

In this work, the H_2O contents of 21 clinopyroxene and garnet inclusions extracted from Canadian diamonds of peridotitic and eclogitic parageneses were investigated using FTIR spectroscopy. The speciation of COH fluids responsible for diamond formation, and the H_2O content of coexisting minerals, have been modelled thermodynamically. The results show that:

- Nominally anhydrous mineral inclusions hosted in Canadian lithospheric diamonds show low H_2O contents compared with the same minerals in xenoliths from the same localities, in agreement with data from other cratonic areas. This indicates that low H_2O activity during diamond formation is a general phenomenon rather than a local curiosity.
- No statistically significant correlations between major/minor element composition and H_2O content for the inclusions, nor for the same minerals from xenoliths, are observed. This suggests that these samples probably underwent a complex polyphase metasomatic history.
- Thermodynamic modelling of a COH fluid at the pressure, temperature and fO_2 conditions along cratonic geotherms shows that, contrary to what was previously thought, COH fluids at the "water maximum" do not occur in the diamond stability field, but rather in the graphite stability field.
- H incorporation models suggest that H_2O contents measured in diamond-hosted NAM inclusions indicate equilibrium with diamond-forming fluids with relatively low H_2O activity.
- According to COH speciation models, and the very low average H_2O content of mineral inclusions, the most common fluids responsible for diamond formation in the lithospheric mantle are carbonatitic and hydrous-carbonated silicate melts.

Funding

This work was supported by the European Union (ERC, INHERIT, Starting Grant No. No 101041620). Views and opinions expressed are, however, those of the author(s) only and do not necessarily reflect those of the European Union or the European Research Council Executive Agency. Neither the European Union nor the granting authority can be held responsible for them.

Conflicts of interest

The authors confirm that this work is original and has not been published elsewhere, nor is it currently under consideration for publication elsewhere.

Use of generative AI

No artificial intelligence tools or services were used to write, construct or organize any part of this manuscript.

CRediT authorship contribution statement

Andrea Curtolo: Conceptualization, Data curation, Formal analysis, Investigation, Methodology, Software, Visualization, Writing – original draft. **Maxwell C. Day:** Investigation, Validation, Writing – review & editing. **Thomas Stachel:** Resources, Validation, Writing – review & editing. **Martha G. Pamato:** Funding acquisition, Writing – review & editing. **Fabrizio Nestola:** Writing – review & editing. **Ingrid L. Chinn:** Resources, Writing – review & editing. **Davide Novella:** Conceptualization, Supervision, Validation, Writing – review & editing.

Declaration of competing interest

The authors declare that they have no known competing financial interests or personal relationships that could have appeared to influence the work reported in this paper.

Acknowledgements

A.C. deeply thanks Dan Frost and Rob Luth for help and discussions regarding the thermodynamic COH speciation model and its implications. The authors thank De Beers Canada Inc. for the provision of the samples from Gahcho Kué Mine. The authors also thank James Badro for editorial handling of the manuscript as well as Jörg Hermann and one anonymous reviewer for providing helpful comments that greatly improved the quality of the manuscript.

Supplementary materials

Supplementary material associated with this article can be found, in the online version, at doi:10.1016/j.epsl.2026.120247.

Data availability

Data can be accessed from the University of Padova online repository at https://researchdata.cab.unipd.it/id/eprint/1887.

References

Aulbach, S., Gies, N.B., Linckens, J., Stalder, R., Viljoen, F., 2024. Inhibited hydrogen uptake in metasomatised cratonic eclogite. Contrib. Mineral. Petrol. 179, 77. https://doi.org/10.1007/s00410-024-02157-6.

Aulbach, S., Stalder, R., Massuyeau, M., Stern, R.A., Ionov, D.A., Korsakov, A.V., 2023. Water in omphacite and garnet from pristine xenolithic eclogite: T-X-fO2 controls, retentivity, and implications for electrical conductivity and deep H2O recycling. Geochem., Geophys., Geosyst. 24, e2023GC011170. https://doi.org/10.1029/2023GC011170.

Aulbach, S., Smart, K.A., 2023. Petrogenesis and geodynamic significance of xenolithic eclogites. Ann. Rev. Earth Planet. Sci. 51, 521–549. https://doi.org/10.1146/annurev-earth-031621.

Balan, E., Paulatto, L., Liu, J., Ingrin, J., 2020. Low-temperature infrared spectrum and atomic-scale structure of hydrous defects in diopside. Eur. J. Mineral. 32, 505–520. https://doi.org/10.5194/ejm-32-505-2020.

Bell, D.R., Ihinger, P.D., Rossman, G.R., 1995. Quantitative analysis of trace OH in garnet and pyroxenes. Am. Mineral. 80, 465–474. https://doi.org/10.2138/am-1995-5-607.

Beyer, C., Frost, D.J., Miyajima, N., 2015. Experimental calibration of a garnet-clinopyroxene geobarometer for mantle eclogites. Contrib. Mineral. Petrol. 169, 18. https://doi.org/10.1007/s00410-015-1113-z.

Bromiley, G.D., Keppler, H., McCammon, C., Bromiley, F.A., Jacobsen, S.D., 2004. Hydrogen solubility and speciation in natural, gem-quality chromian diopside. Am. Mineral. 89, 941–949. https://doi.org/10.2138/am-2004-0703.

Bromiley, G.D, Keppler, H., 2004. An experimental investigation of hydroxyl solubility in jadeite and Na-rich clinopyroxenes. Contrib. Mineral. Petrol. 147, 189–200. https://doi.org/10.1007/s00410-003-0551-1.

Curtolo, A., Condamine, P., Schiavi, F., Bolfan-Casanova, N., Novella, D., 2025b. The effect of CO2 on the partitioning of H2O between clinopyroxene and melts and melting of volatile-bearing eclogites. Geochim. Cosmochim. Acta 398, 54–66. https://doi.org/10.1016/j.gca.2025.03.013.

Curtolo, A., Day, M.C., Innocenzi, F., Bolfan-Casanova, N., Pamato, M.G., Falvard, S., Nestola, F., Harris, J.W., Novella, D., 2025a. H2O in nominally anhydrous mineral inclusions in diamonds and the volatile composition of diamond forming media. Earth Planet. Sci. Lett. 658, 119311. https://doi.org/10.1016/j.epsl.2025.119311.

Curtolo, A., Novella, D., Logvinova, A., Sobolev, N.V., Davies, R.M., Day, M.C., Pamato, M.G., Nestola, F., 2023. Petrology and geochemistry of Canadian diamonds: an up-to-date review. Earth. Sci. Rev. 246, 104588. https://doi.org/10.1016/j.earscirev.2023.104588.

Dasgupta, R., 2018. Volatile-bearing partial melts beneath oceans and continents–where, how much, and of what compositions? Am. J. Sci. 318, 141–165. https://doi.org/10.2475/01.2018.06.

Davies, R.M., Aulbach, S., Stachel, T., 2025. Water and diamond inventory in cratonic eclogite and pyroxenite xenoliths from the Sask and Superior Cratons linked to

tectonomagmatic craton reactivation. Mineral. Petrol. 119, 669–686. https://doi.org/10.1007/s00710-025-00932-2.
Day, M.C., Pamato, M.G., Novella, D., Nestola, F., 2023. Imperfections in natural diamond: the key to understanding diamond genesis and the mantle. La Rivista del Nuovo Cimento 46, 381–471. https://doi.org/10.1007/s40766-023-00045-6.
Dobson, D.P., Jones, A.P., Rabe, R., Sekine, T., Kurita, K., Taniguchi, T., Kondo, T., Kato, T., Shimomura, O., Urakawa, S., 1996. In-situ measurement of viscosity and density of carbonate melts at high pressure. Earth Planet. Sci. Lett. 143, 207–215. https://doi.org/10.1016/0012-821X(96)00139-2.
Donnelly, C.L., Stachel, T., Creighton, S., Muehlenbachs, K., Whiteford, S., 2007. Diamonds and their mineral inclusions from the A154 South pipe, Diavik Diamond Mine, Northwest territories, Canada. Lithos. 98, 160–176. https://doi.org/10.1016/j.lithos.2007.03.003.
Doucet, L.S., Peslier, A.H., Ionov, D.A., Brandon, A.D., Golovin, A.V., Goncharov, A.G., Ashchepkov, I.V., 2014. High water contents in the Siberian cratonic mantle linked to metasomatism: an FTIR study of Udachnaya peridotite xenoliths. Geochim. Cosmochim. Acta 137, 159–187. https://doi.org/10.1016/j.gca.2014.04.011.
Eeken, T., Goes, S., Pedersen, H.A., Arndt, N.T., Bouilhol, P., 2018. Seismic evidence for depth-dependent metasomatism in cratons. Earth Planet. Sci. Lett. 491, 148–159. https://doi.org/10.1016/j.epsl.2018.03.018.
Fagan, A.J., Luth, R.W., 2011. Growth of diamond in hydrous silicate melts. Contrib. Mineral. Petrol. 161, 229–236. https://doi.org/10.1007/s00410-010-0528-9.
Frost, D.J., McCammon, C.A., 2008. The Redox State of earth's mantle. Ann. Rev. Earth Planet. Sci. 36, 389–420. https://doi.org/10.1146/annurev.earth.36.031207.124322.
Gavrilenko, P., 2008. Water solubility in diopside. Ph.D. thesis. University of Bayreuth.
Geiger, C.A., Rossman, G.R., 2018. IR spectroscopy and OH- in silicate garnet: the long quest to document the hydrogarnet substitution. Am. Mineral. 103, 384–393. https://doi.org/10.2138/am-2018-6160CCBY.
Geiger, C.A., Rossman, G.R., 2020a. Micro- and nano-size hydrogarnet clusters and proton ordering in calcium silicate garnet: part I. The quest to understand the nature of "water" in garnet continues. Am. Mineral. 105, 455–467. https://doi.org/10.2138/am-2020-7256.
Geiger, C.A., Rossman, G.R., 2020b. Micro- and nano-size hydrogarnet clusters in calcium silicate garnet: part II. Mineralogical, petrological, and geochemical aspects. Am. Mineral. 105, 468–478. https://doi.org/10.2138/am-2020-7257.
Hasterok, D., Chapman, D.S., 2011. Heat production and geotherms for the continental lithosphere. Earth Planet. Sci. Lett. 307, 59–70. https://doi.org/10.1016/j.epsl.2011.04.034.
Jablon, B.M., Navon, O., 2016. Most diamonds were created equal. Earth Planet. Sci. Lett. 443, 41–47. https://doi.org/10.1016/j.epsl.2016.03.013.
Keppler, H., Bolfan-Casanova, N., 2006. Thermodynamics of water solubility and partitioning. In: Keppler, H., Smyth, J.R. (Eds.), Water in Nominally Anhydrous Minerals. De Gruyter, pp. 193–230. https://doi.org/10.2138/rmg.2006.62.9.
Kessel, R., Pettke, T., Fumagalli, P., 2015. Melting of metasomatized peridotite at 4–6 GPa and up to 1200°C: an experimental approach. Contrib. Mineral. Petrol. 169, 37. https://doi.org/10.1007/s00410-015-1132-9.
Kilgore, M.L., Peslier, A.H., Brandon, A.D., Schaffer, L.A., Morris, R.V., Graff, T.G., Agresti, D.G., O'Reilly, S.Y., Griffin, W.L., Pearson, D.G., Gangi, K., Shaulis, B.J., 2020. Metasomatic control of hydrogen contents in the layered cratonic mantle lithosphere sampled by Lac de Gras xenoliths in the central Slave craton, Canada. Geochimica et Cosmochimica Acta 286, 29–53. https://doi.org/10.1016/j.gca.2020.07.013.
Koch-Müller, M., Abs-Wurmbach, I., Rhede, D., Kahlenberg, V., Matsyuk, S., 2007. Dehydration experiments on natural omphacites: qualitative and quantitative characterization by various spectroscopic methods. Phys. Chem. Miner. 34, 663–678. https://doi.org/10.1007/s00269-007-0181-7.
Koch-Müller, M., Matsyuk, S.S., Wirth, R., 2004. Hydroxyl in omphacites and omphacitic clinopyroxenes of upper mantle to lower crustal origin beneath the Siberian platform. Am. Mineral. 89, 921–931. https://doi.org/10.2138/am-2004-0701.
Kohlstedt, D.L., Keppler, H., Rubie, D.C., 1996. Solubility of water in the α, β and γ phases of (Mg,Fe)2SiO4. Contribution to. Mineral. Petrol. 123, 345–357. https://doi.org/10.1007/s004100050161.
Kovács, I., Green, D.H., Rosenthal, A., Hermann, J., O'Neill, H.S.C., Hibberson, W.O., Udvardi, B., 2012. An experimental study of water in nominally anhydrous minerals in the upper mantle near the water-saturated solidus. J. Petrol. 53, 2067–2093. https://doi.org/10.1093/petrology/egs044.
Krebs, M.Y., Pearson, D.G., Stachel, T., Laiginhas, F., Woodland, S., Chinn, I., Kong, J., 2019. A common parentage-low abundance trace element data of gem diamonds reveals similar fluids to fibrous diamonds. Lithos. 324-325, 356–370. https://doi.org/10.1016/j.lithos.2018.11.025.
Leahy, K., Taylor, W.R., 1997. The influence of the Glennie Domain deep structure on the diamonds in Saskatchewan kimberlites. Russ. Geol. Geophys. 38, 481–491.
Litasov, K.D., Shatskiy, A., Ohtani, E., Yaxley, G.M., 2013. Solidus of alkaline carbonatite in the deep mantle. Geology. 41, 79–82. https://doi.org/10.1130/G33488.1.
Lu, R., Keppler, H., 1997. Water solubility in pyrope to 100 kbar. Contrib. Mineral. Petrol. 129, 35–42. https://doi.org/10.1007/s004100050321.
Luth, R.W., Palyanov, Y.N., Bureau, H., 2022. Experimental petrology applied to natural diamond growth. In: Smit, K., Shirey, S., Pearson, G., Stachel, T., Nestola, F., Moses, T. (Eds.), Diamond: Genesis, Mineralogy and Geochemistry. Mineralogical Society of America, pp. 755–808. https://doi.org/10.2138/rmg.2022.88.1.
Luth, R.W., Stachel, T., 2014. The buffering capacity of lithospheric mantle: implications for diamond formation. Contrib. Mineral. Petrol. 168, 1083. https://doi.org/10.1007/s00410-014-1083-64.
Matsyuk, S.S., Langer, K., Hösch, A., 1998. Hydroxyl defects in garnets from mantle xenoliths in kimberlites of the Siberian platform. Contrib. Mineral. Petrol. 132, 163–179. https://doi.org/10.1007/s004100050414.
Matveev, S., Stachel, T., 2009. Evaluation of kimberlite diamond potential using FTIR spectroscopy of xenocrystic olivine. Lithos. 112, 36–40. https://doi.org/10.1016/j.lithos.2009.04.036.
Mibe, K., Fujii, T., Yasuda, A., 2002. Composition of aqueous fluid coexisting with mantle minerals at high pressure and its bearing on the differentiation of the Earth's mantle. Geochim. Cosmochim. Acta 66, 2273–2285. https://doi.org/10.1016/S0016-7037(02)00856-6.
Mibe, K., Kanzaki, M., Kawamoto, T., Matsukage, K.N., Fei, Y., Ono, S., 2007. Second critical endpoint in the peridotite-H 2 O system. J. Geophys. Res. 112, B03201. https://doi.org/10.1029/2005JB004125.
Mibe, K., Kawamoto, T., Matsukage, K.N., Fei, Y., Ono, S., 2011. Slab melting versus slab dehydration in subduction-zone magmatism. Proc. Natl. Acad. Sci. USA 108, 8177–8182. https://doi.org/10.1073/pnas.1010968108.
Mierdel, K., Keppler, H., 2004. The temperature dependence of water solubility in enstatite. Contrib. Mineral. Petrol. 148, 305–311. https://doi.org/10.1007/s00410-004-0605-z.
Mysen, B.O., 2012. Silicate-COH melt and fluid structure, their physicochemical properties, and partitioning of nominally refractory oxides between melts and fluids. Lithos. 148, 228–246. https://doi.org/10.1016/j.lithos.2012.06.005.
Ni, H., Keppler, H., 2013. Carbon in silicate melts. In: Hazen, R.M., Jones, A.P., Baross, J.A. (Eds.), Carbon in Earth. De Gruyter, pp. 251–287. https://doi.org/10.2138/rmg.2013.75.9.
Nimis, P., 2022. Pressure and temperature data for diamonds. In: Smit, K., Shirey, S., Pearson, G., Stachel, T., Nestola, F., Moses, T. (Eds.), Diamond: Genesis, Mineralogy and Geochemistry. Mineralogical Society of America, pp. 533–565. https://doi.org/10.2138/rmg.2022.88.10.
Nimis, P., Alvaro, M., Nestola, F., Angel, R.J., Marquardt, K., Rustioni, G., Harris, J.W., Marone, F., 2016. First evidence of hydrous silicic fluid films around solid inclusions in gem-quality diamonds. Lithos. 260, 384–389. https://doi.org/10.1016/j.lithos.2016.05.019.
Nimis, P., Taylor, W.R., 2000. Single clinopyroxene thermobarometry for garnet peridotites. Part I. Calibration and testing of a Cr-in-Cpx barometer and an enstatite-in-Cpx thermometer. Contrib. Mineral. Petrol. 139, 541–554. https://doi.org/10.1007/s004100000156.
Novella, D., Bolfan-Casanova, N., Nestola, F., Harris, J.W., 2015. H2O in olivine and garnet inclusions still trapped in diamonds from the Siberian craton: implications for the water content of cratonic lithosphere peridotites. Lithos. 230, 180–183. https://doi.org/10.1016/j.lithos.2015.05.013.
Novella, D., Frost, D.J., 2014. The composition of hydrous partial melts of garnet peridotite at 6GPa: implications for the origin of group II kimberlites. J. Petrol. 55, 2097–2124. https://doi.org/10.1093/petrology/egu051.
O'Leary, J.A., Gaetani, G.A., Hauri, E.H., 2010. The effect of tetrahedral Al3+ on the partitioning of water between clinopyroxene and silicate melt. Earth Planet. Sci. Lett. 297, 111–120. https://doi.org/10.1016/j.epsl.2010.06.011.
O'Reilly, S.Y., Griffin, W.L., 2013. Mantle metasomatism. In: Harlov, D.E., Austrheim, H. (Eds.), Metasomatism and the Chemical Transformation of Rock. Springer, pp. 471–533. https://doi.org/10.1007/978-3-642-28394-9_12.
Padrón-Navarta, J.A., Hermann, J., 2017. A subsolidus olivine water solubility equation for the Earth's upper mantle. J. Geophys. Res. 122, 9862–9880. https://doi.org/10.1002/2017JB014510.
Peslier, A.H., Schönbächler, M., Busemann, H., Karato, S.-I., 2017. Water in the Earth's interior: distribution and origin. Space Sci. Rev. 212, 743–810. https://doi.org/10.1007/s11214-017-0387-z.
Reynes, J., Lanari, P., Hermann, J., 2020. A mapping approach for the investigation of Ti-OH relationships in metamorphic garnet. Contrib. Mineral. Petrol. 175, 46. https://doi.org/10.1007/s00410-020-01681-5.
Schmädicke, E., Gose, J., Stachel, T., 2025. Water in eclogite and pyroxenite xenoliths from the bottom 100 km of the slave craton (Canada) mantle root. Geochem., Geophys., Geosyst. 26, e2024GC011922. https://doi.org/10.1029/2024GC011922.
Shirey, S.B., Cartigny, P., Frost, D.J., Keshav, S., Nestola, F., Nimis, P., Pearson, D.G., Sobolev, N.V., Walter, M.J., 2013. Diamonds and the geology of mantle carbon. In: Hazen, R.M., Jones, A.P., Baross, J.A. (Eds.), Carbon in Earth. Mineralogical Society of America, pp. 355–421. https://doi.org/10.2138/rmg.2013.75.12.
Shirey, S.B., Smit, K.V., Pearson, D.G., Walter, M.J., Aulbach, S., Brenker, F.E., Bureau, H., Burnham, A.D., Cartigny, P., Chacko, T., Frost, D.J., Hauri, E.H., Jacob, D.E., Jacobsen, S.D., Kohn, S.C., Luth, R.W., Mikhail, S., Navon, O., Nestola, F., Nimis, P., Palot, M., Smith, E.M., Stachel, T., Stagno, V., Steele, A., Stern, R.A., Thomassot, E., Thomson, A.R., Weiss, Y., 2019. Diamonds and the mantle geodynamics of carbon. In: Orcutt, B.N., Daniel, I., Dasgupta, R. (Eds.), Deep Carbon: Past to Present. Cambridge University Press, Cambridge, pp. 89–128. https://doi.org/10.1017/9781108677950.005.
Siva-Johty, W., 2020. Studies of inclusions and their host diamonds from the Gahcho Kué mine, Canada. M.Sc thesis. University of Alberta. https://doi.org/10.7939/r3-5y8z-rq94.
Sokol, A.G., Kupriyanov, I.N., Palyanov, Y.N., 2013. Partitioning of H2O between olivine and carbonate-silicate melts at 6.3 GPa and 1400°C: implications for kimberlite formation. Earth Planet. Sci. Lett. 383, 58–67. https://doi.org/10.1016/j.epsl.2013.09.030.
Sokol, A.G., Pal'yanov, Y.N., 2007. Diamond formation in the system MgO–SiO2–H2O–C at 7.5 GPa and 1600°C. Contrib. to Mineral. Petrol. 155, 33–43. https://doi.org/10.1007/s00410-007-0221-9.
Stachel, T., Aulbach, S., Harris, J.W., 2022a. Mineral inclusions in lithospheric diamonds. In: Smit, K., Shirey, S., Pearson, G., Stachel, T., Nestola, F., Moses, T. (Eds.),

Diamond: Genesis, Mineralogy and Geochemistry. Mineralogical Society of America, pp. 307–391. https://doi.org/10.2138/rmg.2022.88.06.
Stachel, T., Cartigny, P., Chacko, T., Pearson, D.G., 2022b. Carbon and nitrogen in mantle-derived diamonds. In: Smit, K., Shirey, S., Pearson, G., Stachel, T., Nestola, F., Moses, T. (Eds.), Diamond: Genesis, Mineralogy and Geochemistry. Mineralogical Society of America, pp. 809–875. https://doi.org/10.2138/rmg.2022.88.15.
Stolper, E., 1982. The speciation of water in silicate melts. Geochim. Cosmochim. Acta 46, 2609–2620. https://doi.org/10.1016/0016-7037(82)90381-7.
Taylor, L.A., Logvinova, A.M., Howarth, G.H., Liu, Y., Peslier, A.H., Rossman, G.R., Guan, Y., Chen, Y., Sobolev, N.V., 2016. Low water contents in diamond mineral inclusions: proto-genetic origin in a dry cratonic lithosphere. Earth Planet. Sci. Lett. 433, 125–132. https://doi.org/10.1016/j.epsl.2015.10.042.
Tollan, P.M.E., O'Neill, H.S.C., Hermann, J., 2018. The role of trace elements in controlling H incorporation in San Carlos olivine. Contrib. Mineral. Petrol. 173, 89. https://doi.org/10.1007/s00410-018-1517-7.
Tollan, P.M.E., Smith, R., O'Neill, H.S.C., Hermann, J., 2017. The responses of the four main substitution mechanisms og H in olivine to H2O activity at 1050°C and 3 GPa. Prog. Earth. Planet. Sci. 4, 14. https://doi.org/10.1186/s40645-017-0128-7.
Weiss, Y., Czas, J., Navon, O., 2022. Fluid inclusions in fibrous diamonds. In: Smit, K., Shirey, S., Pearson, G., Stachel, T., Nestola, F., Moses, T. (Eds.), Diamond: Genesis, Mineralogy and Geochemistry. Mineralogical Society of America, pp. 475–532. https://doi.org/10.2138/rmg.2022.88.09.